A formula for human retinal ganglion cell receptive field density as a function of visual field location

Andrew B. Watson

NASA Ames Research Center, Moffett Field, CA, USA   ✉

In the human eye, all visual information must traverse the retinal ganglion cells. The most numerous subclass, the midget retinal ganglion cells, are believed to underlie spatial pattern vision. Thus the density of their receptive fields imposes a fundamental limit on the spatial resolution of human vision. This density varies across the retina, declining rapidly with distance from the fovea. Modeling spatial vision of extended or peripheral targets thus requires a quantitative description of midget cell density throughout the visual field. Through an analysis of published data on human retinal topography of cones and ganglion cells, as well as analysis of prior formulas, we have developed a new formula for midget retinal ganglion cell density as a function of position in the monocular or binocular visual field.

Introduction

The spatial resolution of human photopic vision is limited by optical blur, and beyond that by spatial sampling by retinal neurons. The initial sampling is by the inner segments of the cone photoreceptors, and subsequent resampling of their signals is performed, via various interneurons, by the retinal ganglion cells (RGC). These are the output cells of the human eye and consequently their properties limit the signal that travels to the rest of the brain. One class of these cells, the midget retinal ganglion cells (mRGC) are the most numerous; near the fovea they appear to sample a single cone while in peripheral retina they gather signals from multiple cones (Ahmad, Klug, Herr, Sterling, & Schein, 2003; Dacey, 1993; Dacey & Petersen, 1992; Goodchild, Ghosh, & Martin, 1996; Kolb & Dekorver, 1991; Schein, 1988). In consequence the mRGC likely set an upper bound on the spatial resolution of human vision, especially at low temporal frequencies (Hirsch & Curcio, 1989; Merigan & Eskin, 1986; Merigan & Katz, 1990; Rossi & Roorda, 2010; Thibos, Cheney, & Walsh, 1987).

From a sampling point of view, the critical metric of the mRGC lattice is the local density or spacing of adjacent mRGC receptive fields (mRGCf). Because this spacing varies across the visual field, and because of its fundamental role in modeling human visual spatial processing, it would be valuable to have a formula for mRGCf spacing as a function of location in the visual field.

An earlier formula for mRGCf density was developed by Drasdo, Millican, Katholi, and Curcio (2007). While this formula was an important contribution, it was largely based on psychophysical results (acuity vs. eccentricity). Since we would like to use our formula to make psychophysical predictions, we sought to develop a formula based only on anatomical data. Barten (1999) also produced a formula for RGC density along an average meridian, but did not provide a derivation for his result.

Dacey (1993) also provided a figure depicting estimated average midget ganglion cell density as a function of eccentricity. However, his estimates are based on highly variable estimates of dendritic field size and an assumption of unit coverage (the product of density and field area) throughout the visual field. Also, separate estimates for the four meridians are not provided. Nonetheless, we show in the Discussion that our new formula is consistent with his empirical results.

The approach that we have taken is to seek a simple analytic formula that approximately satisfies known or probable anatomical constraints.

Curcio, Sloan, Kalina, and Hendrickson (1990) measured the distribution of cone photoreceptors across the retina in a set of eight human eyes. Consistent with earlier fragmentary reports (Osterberg, 1935), they found that density declined rapidly with eccentricity. They also described substantial meridional asymmetries, and large individual differences in peak density.

In a second paper six of those eyes, along with one additional eye, were used to measure the distribution of retinal ganglion cells (Curcio & Allen, 1990). This distribution also varies markedly with eccentricity, but unlike the cone distribution, it does not peak at the fovea. This is because in a central retinal zone the ganglion cell bodies are displaced centrifugally some distance from the inner segments of the cones to which

they are connected through the bipolar cells, and thus from their receptive fields. This displacement zone continues up to eccentricities of around 13°–17°, depending on the meridian (Drasdo et al., 2007). The extent of ganglion cell displacement as a function of eccentricity of the cell body has been measured in primate (Schein, 1988; Wassle, Grunert, Rohrenbeck, & Boycott, 1990) and human (Drasdo et al., 2007). In human these displacements are as large as 2.2°. As a result, the peak RGC density occurs some 4°–5° away from the center of the fovea. Thus the local density of the cell bodies does not reflect the local density of the RGC receptive fields (RGCf).

However, the RGC distribution combined with several other constraints does allow a plausible reconstruction of the distribution of RGCf. The constraints that we consider are:

1. Along a given meridian, the cumulative distribution of RGC and RGCf must agree outside the displacement zone.
2. In the fovea, it is likely that each cone connects (via bipolars) to exactly two mRGC (Kolb & Dekorver, 1991).
3. Near the fovea midgets constitute most but not all of the ganglion cells. The ratio RGC/mRGC is given as about 1.12 by Drasdo et al. (2007).
4. The hypothetical distribution of RGCf must be consistent with the measured distribution of RGC outside of the displacement zone.

Making use of these constraints, this report derives a new formula for RGC density as a function of eccentricity along the four principal meridians, and more generally of position on the retina or in the visual field in degree coordinates.

The derivation relies on transformations from retinal coordinates in mm to degree, based on a model eye (Drasdo & Fowler, 1974) and an assumed offset between optical and visual axes (Charman, 1991), which are described in Appendix 6. We also place in Appendix 5 a number of formulas relating various metrics of points in a hexagonal sampling lattice, such as spacing, density, and row spacing. We also provide (see Appendix 2) with this report a supplementary file of Mathematica functions that implement our formulas (Wolfram Research Inc., 2013). Lastly, we provide a simple interactive demonstration that computes RGCf density and spacing at a selected visual field location (see Appendix 1).

Conventions regarding meridians, locations, and the visual center

In retinal anatomy locations are often specified as a distance from a retinal center along one of the four principal meridians. Because the topography is not radially symmetric, or even bilaterally symmetric, measurements differ along the four meridians. The naming of the meridians is a possible source of confusion, since different conventions are typically used for retinal anatomy and visual fields. Specifically, the nasal retina (the part nearest the nose) images the temporal visual field (the part away from the nose), and vice versa, in both eyes. We avoid this confusion by always referring to the visual field locations, even when discussing anatomy. We order the meridians temporal, superior, nasal, inferior, consistent with increasing polar angle in the visual field of the right eye, and assign them indexes of 1–4. When cartesian coordinates are used, positive x-coordinates refer to the temporal visual field of either eye, or the right binocular visual field.

A further possible confusion is that in the right eye, the temporal visual field is the right visual field, while in the left eye, it is the left visual field. Thus when we compute binocular visual fields, we combine the temporal field of the right eye with the nasal field of the left eye, and vice versa.

A final possible confusion is the definition of the retinal center. Remarkably, there appears to be no consistent term for this concept. What we want is the "visual center," defined essentially as the intersection of the visual axis with the retina. It is not the same as the "fovea" which is an area, not a point. It may well correspond to the point of highest cone density, and is operationally defined as the retinal location that images a fixated point, sometimes called the "preferred retinal locus of fixation" or PRLF (Rossi & Roorda, 2010). We will assume that anatomical measurements and visual field locations are referenced to this common visual center.

Notation

In Appendix 3 we provide a more complete review of notation, but here we introduce some general conventions. The symbol r will indicate eccentricity in degree, d will indicate density in deg^{-2}, and s will indicate spacing (of adjacent cells or receptive fields) in degrees. We use subscripts g, m, and c to denote RGC, mRGC, and cones respectively, and gf and mf to denote RGC and mRGC receptive fields. A particular meridian will be indicated by an integer index k.

Cone densities

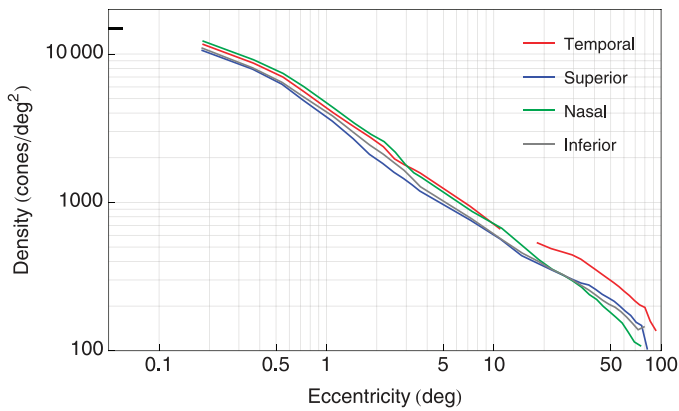Curcio et al. (1990) measured cone photoreceptor density across the retina in eight human eyes. Average

Figure 1. Cone density as a function of eccentricity (Curcio et al., 1990). Foveal density is indicated by the line segment at the upper left. The gap in the temporal meridian corresponds to the blind spot.
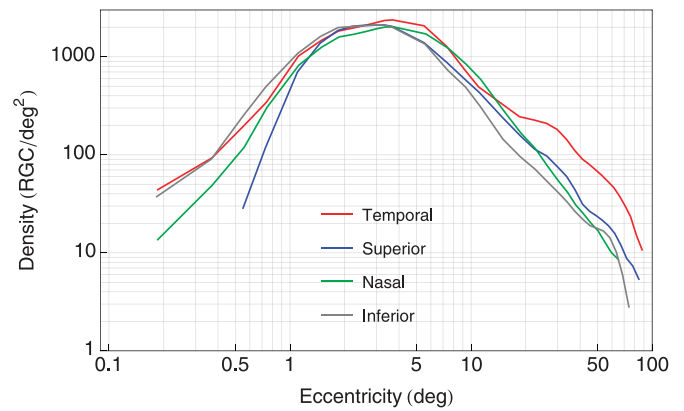

Figure 2. RGC density as a function of eccentricity in four meridians (Curcio & Allen, 1990). The gap in the temporal meridian corresponds to the blind spot.

data are provided in tables of cone densities in cones/mm² in the four principal meridians at each of 34 eccentricities in mm (Curcio, 2006). Using the conversion formulas described in Appendix 6, we have converted the densities to cones/deg² as a function of eccentricity in degree as shown in Figure 1. Writing $d_c(r, k)$ for the cone density at eccentricity r degree along meridian k, we note that the foveal peak is $d_c(0, 1) = d_c(0) = 14,804.6$. This peak density is plotted at the upper left on this log-log plot.

RGC densities

Curcio and Allen (1990) measured local density of RGC cell bodies in seven retinas (including six of those used above to measure cone densities). Curcio (2013) has provided tables of average RGC densities in RGC/mm² in the four principal meridians at each of 35 eccentricities in millimeters. We have again converted these values to densities in RGC/deg² as a function of eccentricity in degree, and the results are plotted in Figure 2. We omit one point in the inferior meridian with a density below 1. The peak density of about 2,375 RGC/deg² occurs not at the foveal center but at an eccentricity of about 3.7°. This is because, as noted above, ganglion cell bodies within a displacement zone extending out as far as 17° are displaced centrifugally from their cone inputs. Thus the RGC densities within this zone cannot be used directly as an estimate of the densities of the RGCf.

The first constraint noted above is that along a given meridian, the cumulative distribution of RGC and RGCf must agree at the limit of the displacement zone. In Figure 3 we show the estimated cumulative number of RGC as a function of eccentricity along each meridian for eccentricities up to 20°. For each meridian,

the counts assume a radially symmetric density function, and are produced through linear interpolation of the data shown in Figure 2. To compute cumulative counts as a function of eccentricity, we integrate density at eccentricity r multiplied by $2\pi r$ to account for the increasing area. The circular point on each curve marks the cumulative density at the approximate limit of the displacement zone (11 for temporal, 17 for the others). When we construct a candidate function for the density of RGCf, its cumulative value must approximately agree at these points. In other words, the total number of receptive fields must equal the total number of cell bodies within the displacement zone.

Foveal density of RGC receptive fields

If each foveal cone drives exactly two midget retinal ganglion cells, as specified in our second constraint,
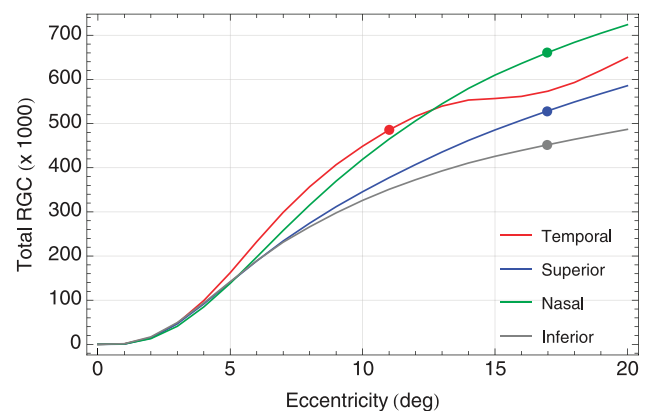

Figure 3. Cumulative total number of RGC along four meridians.

then the foveal density of midget retinal ganglion cell receptive fields must be twice the cone density,

$$d_{mf}(0) = 2d_c(0). \qquad (1)$$

If midget cells constitute a fraction $f(r)$ of all ganglion cells at eccentricity r, then

$$d_{gf}(0) = f(0)^{-1}d_{mf}(0)$$

$$= 2f(0)^{-1}d_c(0) \qquad (2)$$

As noted below, $f(0)^{-1}$ has been estimated as 1.12 (Drasdo et al., 2007) or 1.09 (Dacey, 1993). For reasons outlined below, here we adopt the value of 1.12, in which case $d_{gf}(0) = 2 \times 1.12 \times 14,804.6 = 33,163.2$ deg^{-2}.

Density of RGC receptive fields

We now attempt to discover a function that will describe RGCf density as a function of eccentricity and satisfy the constraints outlined in the Introduction. For each candidate function, we optimized the several parameters with respect to an error function consisting of the sum of the squared errors between empirical and computed log densities for eccentricities outside the exclusion zone, and the weighted squared log of the ratio of empirical and computed cumulative counts within the exclusion zone (see points in Figure 3). This ensures a reasonable fit to peripheral RGC densities, and to the cumulative counts. We used log densities in the fit to accommodate the very wide range of densities, and to avoid giving the larger densities undue influence in the fit. We explored a wide range of functions, leading to the best-fitting one described below.

Since the work of Aubert and Foerster (1857) it has been observed that many measures of visual resolution decline in an approximately linear fashion with eccentricity, at least up to the eccentricity of the blind spot (Strasburger, Rentschler, & Juttner, 2011). Because resolution may depend on receptive field spacing, and since density is proportional to the inverse of spacing squared (see Appendix 5), this suggests that density might vary with eccentricity as

$$d_{gf}(r) = d_{gf}(0)\left(1 + \frac{r}{r_2}\right)^{-2} \qquad (3)$$

where $d_{gf}(0)$ is the density at $r = 0$, and r_2 is the eccentricity at which density is reduced by a factor of four (and spacing is doubled). By itself, this did not provide a good fit, especially at larger eccentricities. However we found that a simple modification, the addition of an exponential, yielded an acceptable fit. The new function is given by

$$d_{gf}(r, k) = d_{gf}(0)$$

$$\times \left[a_k\left(1 + \frac{r}{r_{2,k}}\right)^{-2} + (1 - a_k)\exp\left(-\frac{r}{r_{e,k}}\right) \right] \qquad (4)$$

where a_k is the weighting of the first term, and $r_{e,k}$ is the scale factor of the exponential. The meridian is indicated by the index k. We have fit this expression separately for each meridian and optimized parameters relative to the error function described above. The results are shown in Figure 4. For each meridian, we show the average RGC densities reported by Curcio and Allen (1990), along with the fitted function. The vertical gray line in each figure shows the assumed limit of the displacement zone. Note that only data points outside the displacement zone are used in the fit. The estimated parameters, predicted cell counts, and fitting error are given in Table 1.

The fits are good for three of the four meridians. Both the peripheral densities and the cumulative counts are in close agreement. The agreement is less good for the inferior meridian, largely due to the unusual distribution of the far peripheral densities. The anomalous bump at around 60° and subsequent rapid decline are difficult to fit with simple analytic functions. For comparison, in Figure 5 we show the RGCf density formula in the four meridians, replotted from Figure 4.

RGC displacement

One test of our formula for the density of RGCf is to compare the predicted density of RGC within the displacement zone with the actual densities measured by Curcio and Allen (1990). To generate these predictions we make use of measured displacements from cone inner segment to retinal ganglion cell body in six human retinas along the horizontal meridian (Drasdo et al., 2007). For the separate nasal and temporal meridians, they provided a mathematical formula to describe the average displacement as a function of RGC eccentricity. This can be converted to a function of cone inner segment eccentricity. A difficulty with this function is that it does not provide the correct result at an eccentricity of zero. It should indicate the displacement corresponding to the RGC closest to the fovea, but instead yields a value of 0. Rather than use their formula directly, we have instead constructed a new formula to describe displacement as a function of cone inner segment eccentricity. We constructed this new function to be a reasonable fit to the function of Drasdo but to also yield a displacement of $h(0) > 0°$ at 0° eccentricity. There is some disagreement about the value of $h(0)$. Drasdo stated
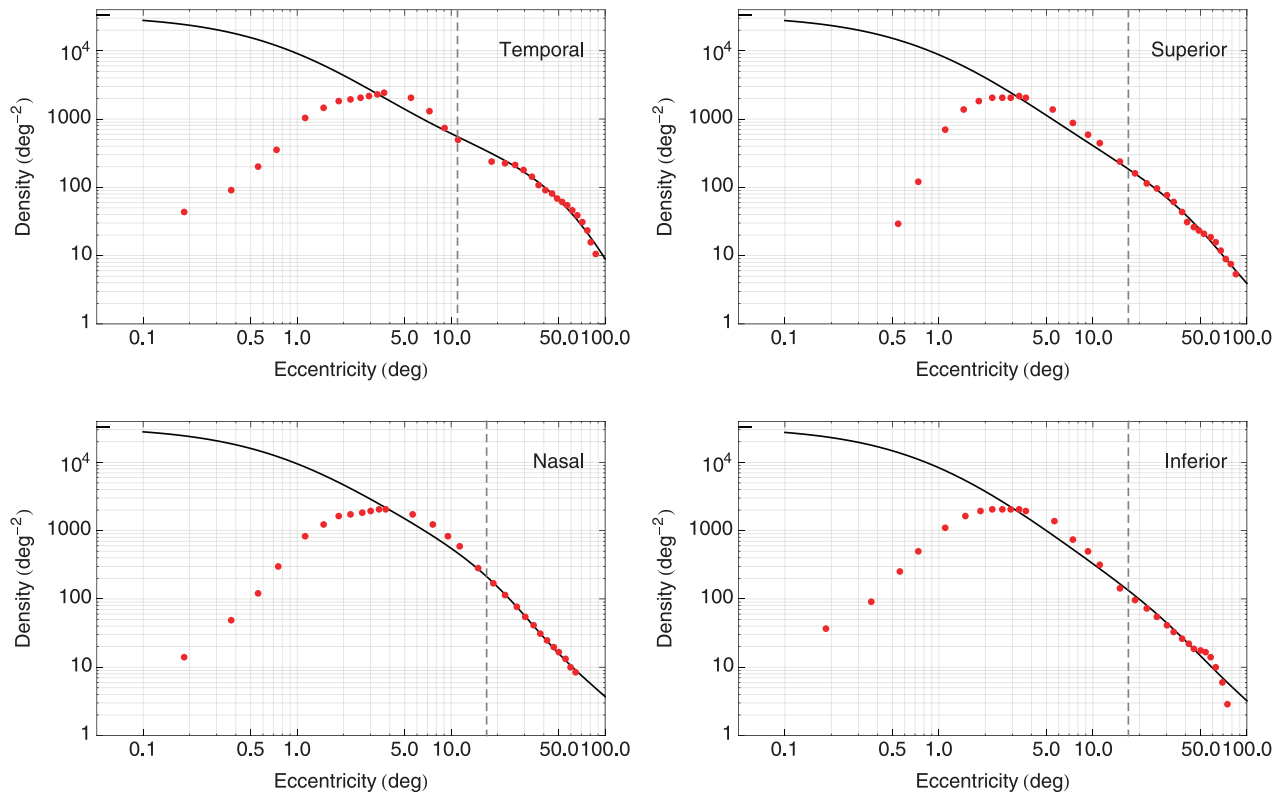
Figure 4. Ganglion cell density as a function of eccentricity in four meridians. Data points are from Curcio and Allen (1990). The solid curve is the fit of Equation 4 to the points outside the displacement zone. The dashed gray line indicates the approximate limit of the displacement zone. The density at eccentricity of zero is indicated by the line segment at the upper left.

that the first RGC are located 0.15 to 0.2 mm (0.53°–0.71°), whereas Curcio provides nonzero RGC densities at eccentricities as small as about 0.2° (see Figure 2). We have assumed a value of 0.5°, but a value of 0.3 gives very similar results.

The displacement function we used is the probability density function of the generalized Gamma distribution (multiplied by the gain δ), given by

$$h(r) = \delta \frac{\gamma e^{-\left(\frac{r-\mu}{\beta}\right)^{\gamma}} \left(\frac{r-\mu}{\beta}\right)^{\alpha\gamma-1}}{\beta \Gamma(\alpha)}. \tag{5}$$

We attach no particular significance to the function or its parameters. It serves only as a device to displace

hypothetical RGC cell bodies, as will be discussed below. This new function is shown in Figure 6, along with the corresponding functions provided by Drasdo for the two meridians. The parameters are provided in Table 2. Note that only three of the parameters are independent, the other two are constrained by the value of $h(0)$ and by the peak value, which we set to the maximum of the fitted values.

Next we generated a population of RGC with eccentricities based on our density formula (Equation 4). Eccentricities were random within annuli of 0.05°. We then displaced each RGC centrifugally according to the displacement function (Equation 5, Figure 6). The density of the displaced cells was then computed.

Meridian	k	a	r_2	r_e	Data count (× 1000)	Model count (× 1000)	Error	r_z
Temporal	1	0.9851	1.058	22.14	485.1	485.7	0.23	11
Superior	2	0.9935	1.035	16.35	526.1	528.9	0.12	17
Nasal	3	0.9729	1.084	7.633	660.9	661.1	0.01	17
Inferior	4	0.996	0.9932	12.13	449.3	452.1	0.93	17

Table 1. Parameters and error for fits of Equation 4 in four meridians. Note: Also shown are measured and predicted cumulative counts along each meridian within the displacement zone. The next-to-last column shows the fitting error outside the displacement zone. The last column indicates the assumed limit of the displacement zone.
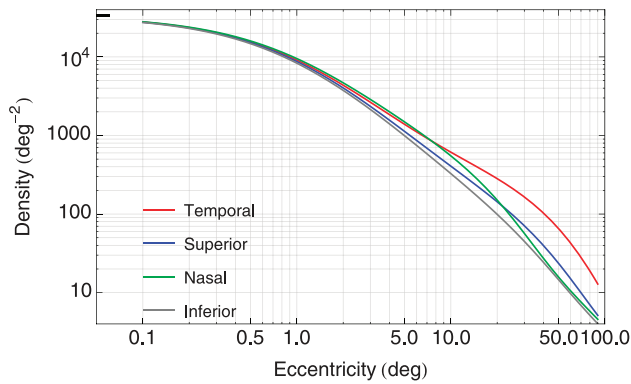
Figure 5. RGCf density formula as a function of eccentricity for four meridians, replotted from Figure 4.

Results are shown in Figure 7. Note that this test can only be conducted on the two horizontal meridians along which displacement was measured. The actual and predicted densities are in reasonable agreement. In one case, the peak densities are too low and in the other, too high, but the height and shape of the distributions are approximated. Note that the displacements and densities were estimated from a different (but overlapping) set of eyes, and thus complete agreement is not expected.

Midget RGCf density

   Midget cells make up most but not all of the retinal ganglion cells, and their proportion varies with eccentricity. In general, the density of midget retinal ganglion cell receptive fields is given by

$$d_{mf}(r, k) = f(r)d_{gf}(r, k) \qquad (6)$$

where $f(r)$ is the fraction of retinal ganglion cells that

are midgets, as introduced in Equation 2. Two estimates of $f(r)$ have been provided in the literature.

   Dacey (1993) estimated mRGC dendritic field diameters at various eccentricities in whole mounts of human retina. Careful examination of dendritic trees at several midperipheral and peripheral locations indicated a coverage (dendritic field area × density) of approximately 1. By assuming that this coverage remained constant at 1 throughout the retina Dacey estimated the density of midget cells as the inverse of dendritic field area. The ratio of that density to Curcio and Allen's (1990) estimates of RGC density (beyond about 3.5°) provided an estimate of the fraction of RGC that are midget cells. These estimates of Dacey are shown as the points in Figure 8. They range from over 95% near the fovea to less than 50% in the far periphery.

   A second estimate of $f(r)$ was provided by Drasdo et al. (2007) as the formula

$$f(r) = f(0)\left(1 + \frac{r}{r_m}\right)^{-1} \qquad (7)$$

where $f(0) = 1/1.12 = 0.8928$ and $r_m = 41.03°$. The formula is shown by the curve in Figure 8. This formula was derived from iterative fit of a more elaborate expression involving both psychophysical measures and anatomical measures (Drasdo et al., 2007). Drasdo and Dacey's measures agree generally that the fraction declines with eccentricity, and roughly agree in foveal and peripheral asymptotes.

   One problem with Dacey's method is that from about 3.5° to 17° it includes both RGC densities and dendritic field measurements of displaced cells. Hence his estimates at those eccentricities may not reflect the fraction of receptive fields belonging to midget cells. For this reason, and until better estimates can be obtained, we adopt Drasdo's formula to compute the density of mRGCf. Combining Equations 2, 4, 6, and 7, we have
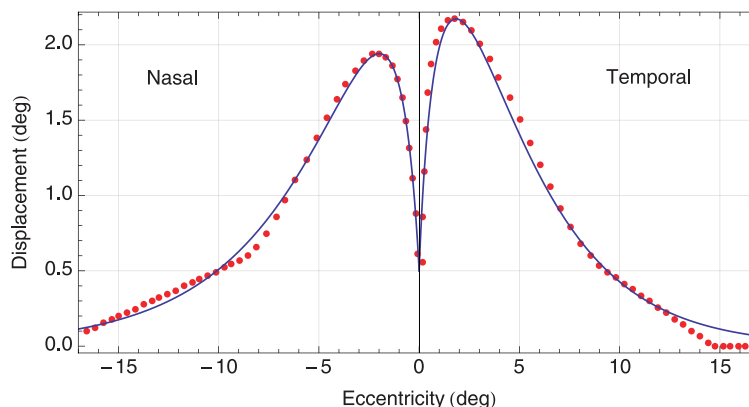

Figure 6. Modeled displacement functions (solid curve) and points from the formula of Drasdo et al. (2007).

Meridian	α	"β(deg)	γ	δ	μ(deg)
Temporal	1.8938	2.4598	0.91565	14.904	−0.09386
Nasal	2.4607	1.7463	0.77754	15.111	−0.15933

Table 2. Parameters of the displacement function (Equation 5 and Figure 6).

$$d_{mf}(r,k) = 2d_c(0)\left(1 + \frac{r}{r_m}\right)^{-1}$$
$$\times \left[a_k\left(1 + \frac{r}{r_{2,k}}\right)^{-2} + (1 - a_k)\exp\left(-\frac{r}{r_{e,k}}\right)\right]. \quad (8)$$

This formula is plotted in Figure 9 for the four meridians.

mRGCf spacing

On the assumption of hexagonal packing (Equation A4), the spacing of adjacent midget receptive fields is given by

$$s_{mf}(r,k) = \sqrt{\frac{2}{\sqrt{3}d_{mf}(r,k)}}. \quad (9)$$

Spacing at a binocular horizontal eccentricity can be computed by averaging densities at corresponding eccentricities in temporal and nasal meridians and converting to spacing. We can also compute the "mean" spacing, the average of all four meridians, by averaging densities and converting to spacing. These formulas for spacing are plotted in Figure 10. We show the individual meridians and the "Horizontal" and "Mean" versions.

Note that the midget RGC are composed of approximately equal numbers of "on" and "off" center cells (we neglect reports of asymmetry between the two types). Typically we are concerned with the spacing within one class, in which case density is halved and the spacings should be multiplied by $\sqrt{2}$. In Figure 11 we show the formula scaled in this way for eccentricities between 0° and 10°, and we express the spacings in arcmin.

Averaged across meridians, the computed spacing of mRGCf is very nearly linear ($R^2 = 0.9997$). This allows us to write the following simple approximation for average spacing in either on- or off-center mosaic, where both s and r are expressed in degrees.

$$60s = 0.53 + 0.434r \quad (10)$$

This convenient result is the due to the form of Equation 4, and the fact that the second exponential term does not have much effect for eccentricities less than 30°.

Extension to arbitrary retinal locations

To this point we have developed formulas describing spacing as a function of eccentricity along each of the four principal meridians. We would like to extend these formulas to describe spacing at an arbitrary point $\{x, y\}$ in the retina. To do this we make the assumption that within any one quadrant of the retina the iso-spacing contours are ellipses. This is consistent with the idea that spacing changes smoothly with the angle of a ray extending from the visual center. An example is shown in Figure 12. The eccentricities at the intersections of the ellipse with the two enclosing meridians are r_x and r_y.

Under the ellipse assumption, we can write

$$\left(\frac{x}{r_x}\right)^2 + \left(\frac{y}{r_y}\right)^2 = 1 \quad (11)$$
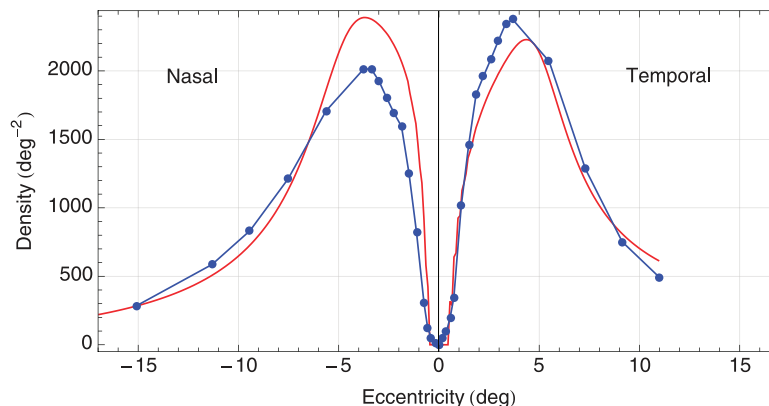

Figure 7. Modeled and measured density of displaced retinal ganglion cells in temporal (left) and nasal (right) meridians.
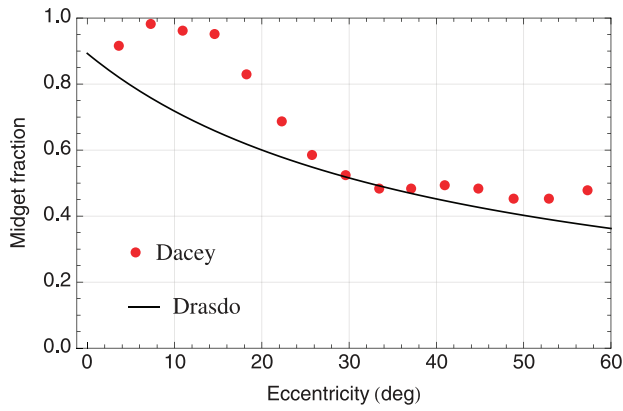
Figure 8. Estimated fraction of RGC that are midget cells as a function of eccentricity.

Figure 10. Formula for mRGCf spacing.

And because they are on an iso-spacing curve,

$$s(r_x, 1) = s(r_y, 2) \tag{12}$$

Given numerical values for x and y, we can solve Equations 11 and 12 together to find numerical solutions for r_x and r_y, and then we can compute

$$s(\{x, y\}) = s(r_x, 1) \tag{13}$$

To avoid solving a system of equations, we have found that the following approximation works well. Let r_{xy} be the radial eccentricity of the point $\{x, y\}$,

$$r_{xy} = \sqrt{x^2 + y^2} \tag{14}$$

Then we compute

$$s(\{x, y\}) = \sqrt{\left(\frac{x}{r_{xy}} s(r_{xy}, 1)\right)^2 + \left(\frac{y}{r_{xy}} s(r_{xy}, 2)\right)^2}$$

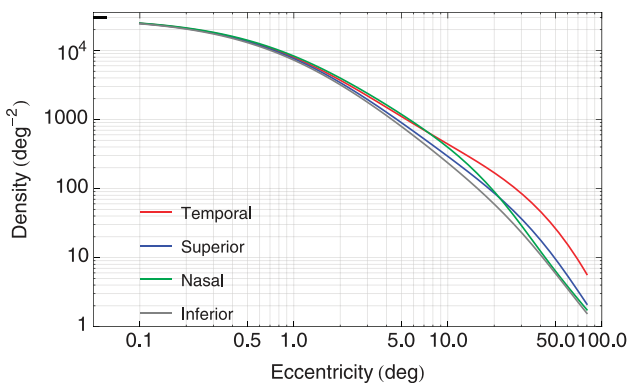$$= \frac{1}{r_{xy}} \sqrt{x^2 s(r_{xy}, 1)^2 + y^2 s(r_{xy}, 2)^2} \tag{15}$$
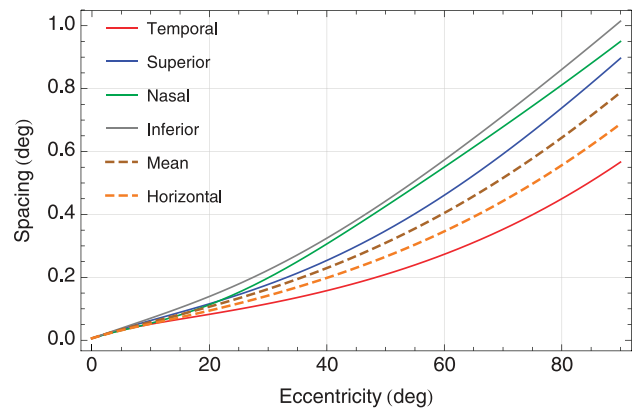
This approximation is always within 1.7% of the value obtained by Equations 10 through 12. Equation 15 is easily generalized to work for arbitrary retinal quadrants. Since the sign of the horizontal coordinate is arbitrary, we define positive x values to mean the temporal visual field. This corresponds to the right visual field for the right eye, and the left visual field for the left eye.

Extension to arbitrary binocular visual field locations

Equation 15 computes mRGC spacing at locations specified in visual field coordinates in one eye. In psychophysical modeling of natural vision, it is useful to compute spacing at locations specified in the binocular visual field. To do this we compute the spacing at corresponding visual field locations in the

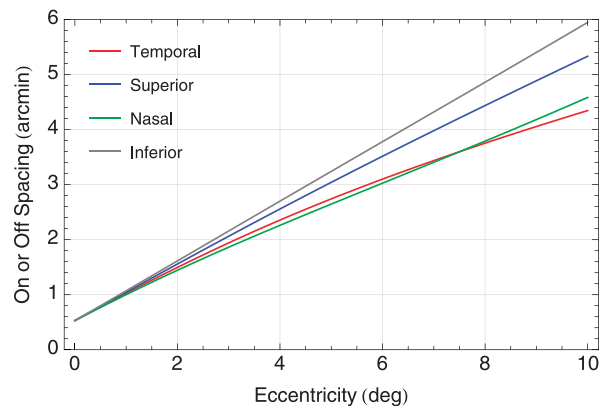Figure 9. mRGCf density formula as a function of eccentricity (Equation 8).

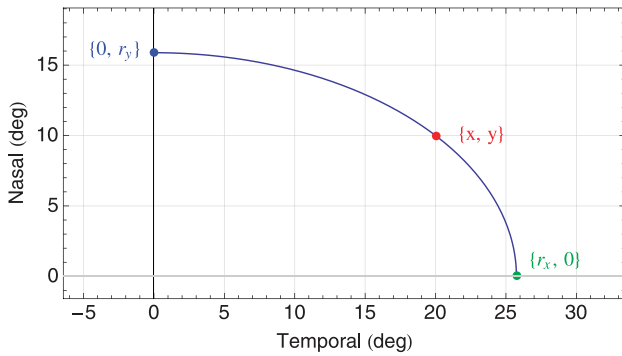Figure 11. Formula for on or off mRGCf spacing for eccentricities 0°–10°.

Figure 12. A hypothetical iso-spacing curve in one quadrant, including a point {x, y} and points on the two enclosing meridians.

two eyes, convert them to densities (Equation 2), compute their mean, and convert back to spacing (Equation A4). After simplifying, we obtain the following result for binocular spacing s_B:

$$s_B(\{x, y\}) = \sqrt{2}\sqrt{\frac{s(\{-x, y\})^2 s(\{x, y\})^2}{s(\{-x, y\})^2 + s(\{x, y\})^2}}. \quad (16)$$

With this function we can compute a plot of the Nyquist frequency over the binocular visual field, as shown in Figure 13. In this calculation we have divided the value by $\sqrt{2}$, based on the assumption of overlapping lattices of on- and off-center cells. The peak value is 65.4 cycles/deg. Because there is some ambiguity about the best way to combine the densities of the two eyes, in our supplementary materials we also provide functions that compute the maximum density, or the total density of the two eyes.

Discussion

Ratio of midget RGC and cones

In Figure 14 we plot the ratio between mRGCf densities computed from Equation 8 and cone densities reported by Curcio et al. (1990). Although we did not impose this as a constraint in estimating a function for the density of ganglion cells, the ratio remains close to 2 for the central several degrees. This is roughly consistent with Dacey's report that up to about 4° mRGC dendritic fields remain at a minimum size appropriate to connection with a single bipolar, and thereby to a single cone. Beyond about 6°, he found that dendritic fields enlarge and begin to show clusters suggesting input from multiple cones, and consistent with the decline in the ratio in Figure 14. Our result is also consistent with Schein's estimate that the ratio remains constant out to about 2.5° in primates (Schein, 1988).

Comparison with Drasdo et al. (2007)

In Figure 15 we compare mRGCF spacing computed from our formula to densities computed from the formula of Drasdo et al. (2007), converted to spacings by Equation A4. While there is considerable agreement, there are some significant discrepancies. In particular the curves for the superior and inferior meridians are nearly interchanged in the two formulas. Our formula is consistent with Curcio and Allen (1990) who clearly show higher density (smaller spacing) in superior versus inferior meridians beyond about 6° (see Figure 2), while
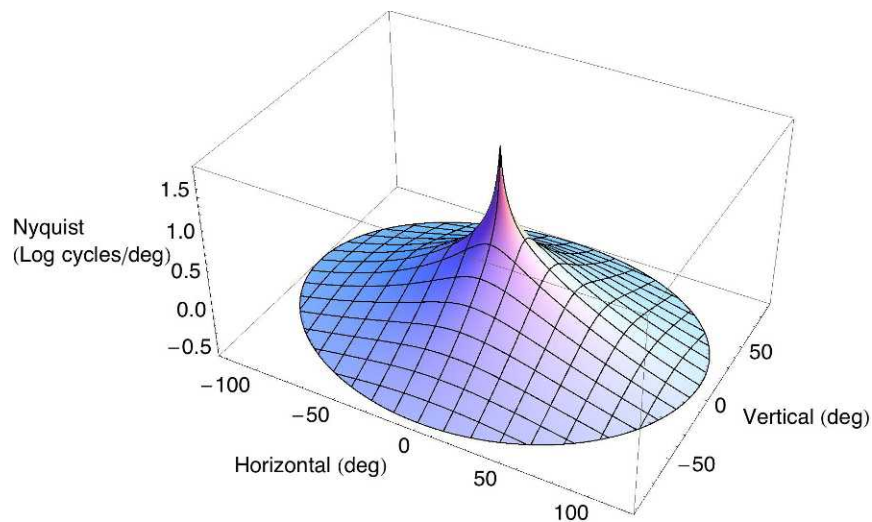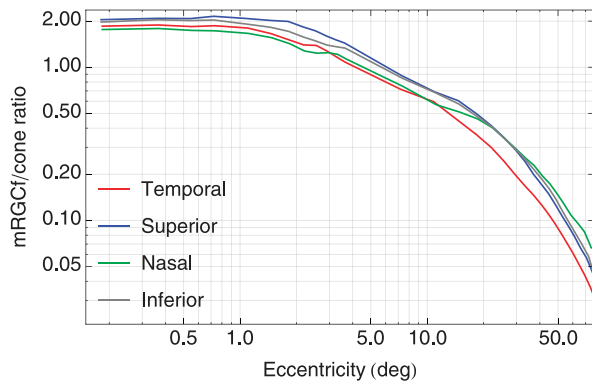

Figure 13. Nyquist frequency over the binocular visual field based on the density formula and assuming separate and equal on- and off-center populations.

Figure 14. Ratio of mRGCf to cones as a function of eccentricity based on the Watson formula for mRGCf density.

Drasdo's formula shows the opposite, for unknown reasons. We also note that the Drasdo formula is defined only up to 30°, while ours extends at least as far as 90°.

Comparison with dendritic field diameter

Dacey measured dendritic field diameters of midget ganglion cells in human retina (Dacey, 1993; Dacey & Petersen, 1992). In Figure 16 we have reproduced his Figure 4B, that shows diameter as a function of eccentricity. The filled points are for the temporal quadrant, open points are for the other quadrants. Near the fovea, where mRGC connect to single cone, we do not expect any relationship between field diameter and cell spacing. However in the periphery, Dacey found that within either the on- or off-center lattice, spacing and diameter were about equal. This allows us to compare his measures of diameter to our spacing formula for equivalent eccentricities and quadrants. Formula values for the temporal meridian and the mean of the other three meridians are shown by
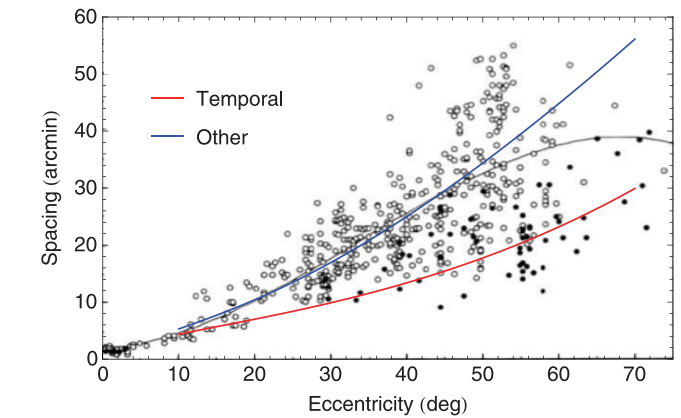

Figure 16. Dendritic field diameter as a function of eccentricity for human mRGC as measured by Dacey (1993). Filled points are for the temporal meridian; open points are for other quadrants. Gray curve is Dacey's estimate of the mean. Red and blue curves show spacing calculated from our formula for the temporal meridian or the mean of the other meridians.

the colored curves in Figure 16. The computed spacing is for either the on- or off-center lattice. The agreement is reasonable, especially considering the sizable scatter in measurements of diameter.

Comparison with acuity

Rossi and Roorda (2010) provide estimates of letter acuity, expressed as minimum angle of resolution (MAR) for five observers viewing targets under adaptive optics conditions. The targets were at nasal visual field locations between 0° and 2.5°. In Figure 17 we compare their results with the computed row spacing, assuming separate on- and off-cell lattices. We use separate lattices on the assumption that, at least near the fovea, both an on and an off midget cell are required to signal the signed value of local contrast. In
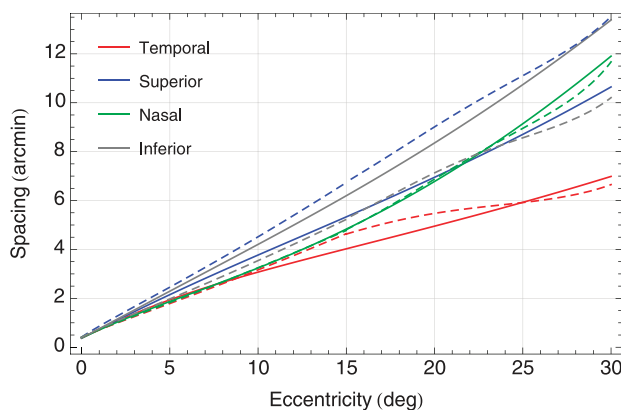

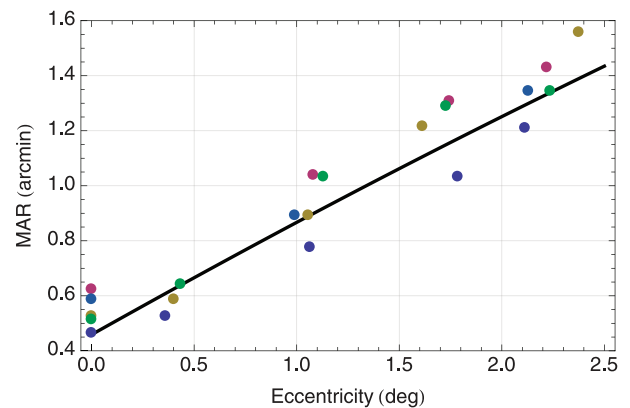Figure 15. Comparison of formulas of Watson and Drasdo et al. (2007) (dashed).

Figure 17. Human letter acuity (points) along the nasal meridian of five observers from Rossi and Roorda (2010) and row spacing from our formula for the same meridian (line).
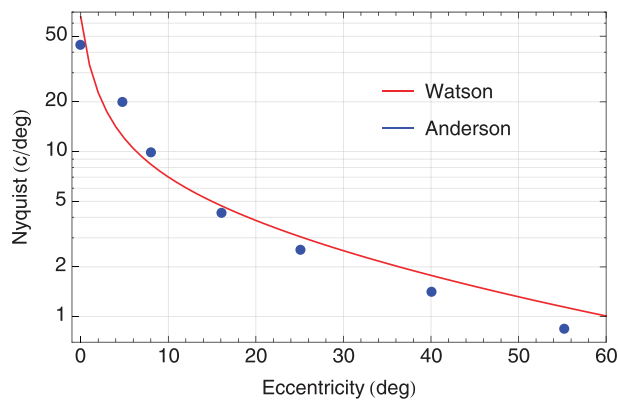
Figure 18. Human grating acuity (points) from Anderson et al. (1991) and calculated Nyquist frequency of midget RGC.

addition, where each cone drives one on and one off midget, we know the two midgets have the same receptive field location. Specifically, the function returned by Equation 9 is multiplied by $60 \sqrt{2} \sqrt{3} / 2 = 30 \sqrt{6}$ to reflect the halved density, conversion to row spacing, and conversion to arcmin. The agreement is excellent. This is not surprising, since Rossi and Roorda previously showed good agreement with the formula of Drasdo et al. (2007), to which ours is similar for small eccentricities.

Estimates of peripheral acuity are complicated by the possibility of aliasing. Anderson, Mullen, and Hess (1991) attempted to bypass this problem by using direction discrimination of drifting gratings. Their results are plotted in Figure 18, along with calculations of Nyquist frequency of the on- or off-center mRGCf lattice from Equations 8 and A3. The agreement is reasonable. One caveat regarding the comparison at $r = 0$ is that these data were collected with Gabor targets that extended (at half height) well over 0.5°, so that performance may reflect the averaging spacing over that area. The precise relationship between mRGCf spacing and acuity is beyond the scope of this paper (Anderson & Thibos, 1999), here we only point to the general agreement in both the shape and absolute level of the calculations.

Comparison with Sjöstrand

In a series of papers Sjöstrand, Popovic, and colleagues measured human RGC densities at eccentricities from about 2° to 34° eccentricity along the vertical meridian in sectioned human retinas (Popovic & Sjöstrand, 2001, 2005; Sjöstrand, Olsson, Popovic, & Conradi, 1999; Sjostrand, Popovic, Conradi, & Marshall, 1999). From these densities, using their own estimates of displacement, the inferred RGC spacing at various eccentricities. Their formula for conversion

from density to spacing actually yields the row spacing (Equation A1) not the spacing between cells (Equation A4), which is $2 / \sqrt{3}$ larger. Even taking this into account, their values are about a factor 0.75 smaller than those computed from our formula for the mean of superior and inferior meridians. However their values are also discrepant with Drasdo's formula (Figure 6) and with spacing estimated from Dacey's estimates of mRGC field diameter (Figure 16). Some part of this discrepancy may arise from their formula for displacement, which though similar in form is only half the magnitude of ours or that of Drasdo, who has also commented on this discrepancy (Drasdo et al., 2007).

Popovic and Sjöstrand (2005) measured acuity of three observers at eccentricities between 5.8° and 26.4° in both eyes, one of which was subsequently enucleated. Ganglion cell densities and spacings were measured along the vertical meridian. Acuity (MAR) was measured using high-pass resolution perimetry. They found MAR was approximately proportional to RGC spacing over the full range of eccentricities. The constant of proportionality was rather large (4.24), especially compared to the value of 1 we have used in Figures 17 and 18. They note that correcting for the low contrast of their target (0.25), and considering only spacing in one class (on or off) of midget cells as we have done, would lower the constant to 1.43. The remaining discrepancy may be due to their low estimates of spacing, as noted above. In general, their results support the notion that psychophysical resolution is governed by the mRGC spacing.

Midget fraction

Perhaps the least secure element of our formula is the midget fraction, the function describing the fraction of all ganglion cells that are midget as a function of eccentricity. As noted above (Figure 8) there are discrepancies between available estimates. We have adopted the formula of Drasdo, but it is unclear whether that is accurate, especially at very large eccentricities, where it continues to descend to values as low as 0.25. In the periphery, where his estimates are arguably most accurate, Dacey's estimates appear the level off at about 0.5. Until more definitive estimates are available, we will have to acknowledge the speculative nature of this element.

Variability

I have based my formula on average densities of cones and retinal ganglion cells (Curcio & Allen,

1990; Curcio et al., 1990). Curcio et al. (1990) note a very large variation in peak cone density in their set of nine eyes, ranging from 98,200 to 324,100 mm^{-2} (7,385 to 24,372 deg^{-2}) (coefficient of variation ~0.46). When two anomalous eyes are excluded, the lower bound only increases to 166,000 mm^{-2} (12,483 deg^{-2}). This variation largely disappeared at eccentricities beyond 1°, so that the total number of cones within a radius of about 3.6° (or over the entire retina) was nearly constant (coefficient of variation ~0.1). However, more recent density estimates from in vivo measurement show a fairly consistent coefficient of variation (~0.2) regardless of eccentricity (Song, Chui, Zhong, Elsner, & Burns, 2011). These latter authors have also shown an up to 25% decrement in density with age, primarily at eccentricities less than 1.6°. Curcio's data, and our formula, are consistent with the data for their younger group of observers.

Ganglion cell densities also show sizable individual differences (Curcio & Allen, 1990). However, perhaps in contrast to cones, the total number varies considerably, from 0.71 to 1.54 million cells over a set of six eyes. This variation seems to be consistent across the retina. Variation at the fovea cannot be directly determined because of the displacement of the RGC.

Beyond these variations between individuals and with respect to age, there may be additional sources of variability and measurement error. Thus while a formula for the average may be useful, it is important to note that individuals may differ considerably from these computed values.

Conclusions

We have derived a mathematical formula for the density of receptive fields of human retinal ganglion cells as a function of position in the monocular or binocular visual field. Densities can also be computed for the receptive fields of the midget subclass of ganglion cells. Both spacing and position are expressed in degrees. The formula has several advantages over existing formulas, which are based on psychophysics, limited to small eccentricities, confined to specific meridians, or are inaccurate in the foveal region. Since the midget retinal ganglion cells provide the primary limit on human visual spatial resolution across the visual field, this formula may be useful in the modeling of human spatial vision.

Keywords: vision, perception, acuity, retinal topography, retinal ganglion cells, midget retinal ganglion cell, eccentricity, peripheral vision, visual resolution

Acknowledgments

Commercial relationships: none.
Corresponding author: Andrew B. Watson.
Email: andrew.b.watson@nasa.gov.
Address: NASA Ames Research Center, Moffett Field, CA, USA.

References

Ahmad, K. M., Klug, K., Herr, S., Sterling, P., & Schein, S. (2003). Cell density ratios in a foveal patch in macaque retina. *Visual Neuroscience*, *20*(2), 189–209.

Anderson, R. S., & Thibos, L. N. (1999). Relationship between acuity for gratings and for tumbling-E letters in peripheral vision. *Journal of the Optical Society of America A*, *16*(10), 2321–2333, http://josaa.osa.org/abstract.cfm?URI=josaa-16-10-2321.

Anderson, S. J., Mullen, K. T., & Hess, R. F. (1991). Human peripheral spatial resolution for achromatic and chromatic stimuli: Limits imposed by optical and retinal factors. *Journal of Physiology*, *442*, 47–64, http://www.ncbi.nlm.nih.gov/pubmed/1798037.

Aubert, H. R., & Foerster, C. F. R. (1857). Beiträge zur Kenntniss des indirecten Sehens. (I). Untersuchungen über den Raumsinn der Retina [Translation: Contributions to the knowledge of the indirect vision: I. Studies on the sense of space of the retina]. *Archiv für Ophthalmologie*, *3*, 1–37.

Barten, P. G. J. (1999). *Contrast sensitivity of the human eye and its effects on image quality*. Bellingham, WA: SPIE Optical Engineering Press.

Charman, W. N. (1991). Optics of the human eye. In J. Cronly Dillon (Ed.), *Visual optics and instrumentation* (pp. 1–26). Boca Raton: CRC Press.

Curcio, C. (2006). 4meridians.xls. Retrieved from http://www.cis.uab.edu/sloan/PRtopo/4meridians.xls.

Curcio, C. (2013). Curcio_JCompNeurol1990_GCtopo_F6.xls.

Curcio, C. A., & Allen, K. A. (1990). Topography of ganglion cells in human retina. *Journal of Comparative Neurology, 300*(1), 5–25.

Curcio, C. A., Sloan, K. R., Kalina, R. E., & Hendrickson, A. E. (1990). Human photoreceptor topography. *Journal of Comparative Neurology, 292*(4), 497–523, http://www.ncbi.nlm.nih.gov/pubmed/2324310.

Dacey, D. M. (1993). The mosaic of midget ganglion cells in the human retina. *Journal of Neuroscience, 13*(12), 5334–5355, http://www.ncbi.nlm.nih.gov/pubmed/8254378.

Dacey, D. M., & Petersen, M. R. (1992). Dendritic field size and morphology of midget and parasol ganglion cells of the human retina. *Proceedings of the National Academy of Sciences, USA, 89*(20), 9666–9670, http://www.ncbi.nlm.nih.gov/pubmed/1409680.

Drasdo, N., & Fowler, C. W. (1974). Non-linear projection of the retinal image in a wide-angle schematic eye. *British Journal of Ophthalmology, 58*(8), 709–714, http://www.ncbi.nlm.nih.gov/pubmed/4433482.

Drasdo, N., Millican, C. L., Katholi, C. R., & Curcio, C. A. (2007). The length of Henle fibers in the human retina and a model of ganglion receptive field density in the visual field. *Vision Research, 47*(22), 2901–2911, http://www.ncbi.nlm.nih.gov/pubmed/17320143.

Emsley, H. H. (1952). *Visual optics* (5th ed.). London: Hatton Press.

Goodchild, A. K., Ghosh, K. K., & Martin, P. R. (1996). Comparison of photoreceptor spatial density and ganglion cell morphology in the retina of human, macaque monkey, cat, and the marmoset *Callithrix jacchus. Journal of Comparative Neurology, 366*(1), 55–75, http://www.ncbi.nlm.nih.gov/pubmed/8866846.

Hirsch, J., & Curcio, C. A. (1989). The spatial resolution capacity of human foveal retina. *Vision Research, 29*(9), 1095–1101.

Kolb, H., & Dekorver, L. (1991). Midget ganglion cells of the parafovea of the human retina: A study by electron microscopy and serial section reconstructions. *Journal of Comparative Neurology, 303*(4), 617–636, http://www.ncbi.nlm.nih.gov/pubmed/1707423.

Merigan, W. H., & Eskin, T. A. (1986). Spatiotemporal vision of macaques with severe loss of P-beta retinal ganglion cells. *Vision Research, 26,* 1751–1761.

Merigan, W. H., & Katz, L. M. (1990). Spatial resolution across the macaque retina. *Vision Research, 30*(7), 985–991.

Osterberg, G. A. (1935). Topography of the layer of rods and cones in the human retina. *Acta Ophthalmologica, 6*(Suppl. VI), 1–97.

Popovic, Z., & Sjöstrand, J. (2005). The relation between resolution measurements and numbers of retinal ganglion cells in the same human subjects. *Vision Research, 45*(17), 2331–2338.

Popovic, Z., & Sjöstrand, J. (2001). Resolution, separation of retinal ganglion cells, and cortical magnification in humans. *Vision Research, 41*(10), 1313–1319.

Rossi, E. A., & Roorda, A. (2010). The relationship between visual resolution and cone spacing in the human fovea. *Nature Neuroscience, 13*(2), 156–157, http://dx.doi.org/10.1038/nn.2465.

Schein, S. J. (1988). Anatomy of macaque fovea and spatial densities of neurons in foveal representation. *Journal of Comparative Neurology, 269*(4), 479–505, http://www.ncbi.nlm.nih.gov/pubmed/3372725.

Sjöstrand, J., Olsson, V., Popovic, Z., & Conradi, N. (1999). Quantitative estimations of foveal and extra-foveal retinal circuitry in humans. *Vision Research, 39*(18), 2987–2998.

Sjostrand, J., Popovic, Z., Conradi, N., & Marshall, J. (1999). Morphometric study of the displacement of retinal ganglion cells subserving cones within the human fovea. *Graefes Archives for Clinical & Experimental Ophthalmology, 237*(12), 1014–1023.

Song, H., Chui, T. Y. P., Zhong, Z., Elsner, A. E., & Burns, S. A. (2011). Variation of cone photoreceptor packing density with retinal eccentricity and age. *Investigative Ophthalmology & Visual Science, 52*(10), 7376–7384, http://www.iovs.org/content/52/10/7376. [Pubmed] [Article]

Strasburger, H., Rentschler, I., & Juttner, M. (2011). Peripheral vision and pattern recognition: A review. *Journal of Vision, 11*(5):13, 1-82, http://www.journalofvision.org/content/11/5/13, doi:10.1167/11.5.13. [Pubmed] [Article]

Thibos, L., Cheney, F., & Walsh, D. (1987). Retinal limits to the detection and resolution of gratings. *Journal of the Optical Society of America A, 4*(8), 1524–1529.

Wassle, H., Grunert, U., Rohrenbeck, J., & Boycott, B. B. (1990). Retinal ganglion cell density and cortical magnification factor in the primate. *Vision Research, 30*(11), 1897–1911, http://www.ncbi.nlm.nih.gov/pubmed/2288097.

Wolfram Research Inc. (2013). *Mathematica* (Version 9.0). Champaign, IL: Author.

Retinal Topography Calculator

Location =   {0, 0}   deg

| Density = | 29609.3 deg^{-2} | Spacing = | 0.375 | arcmin |
| Row spacing = | 0.324 arcmin | Nyquist = | 92.5 | cycles/deg |

Visual field ⦿ binocular–mean ○ binocular–best ○ binocular–total ○ right eye

Midget only ☑

On+Off ☑

Reset ☐

x = 0 ——●——

y = 0 ——●——

This calculator computes density and spacing of human retinal ganglion cells based on the formula of Watson (2014).
   This demonstration is included as a supplement to the paper: Watson, A. B., (2014). A formula for human retinal ganglion cell
   receptive field density as a function of visual field location. Journal of Vision, 14(7), http://www.journalofvision.org/content/14/7.toc.
   Definition of the formula can be found there. Copyright Andrew B. Watson. Date of this version: 2014/6/26.
Instructions: Drag the cross–hairs in the graphic at the top, or the siders in the controls below, to specify the visual field location.
   Values of ganglion cell density, spacing, row spacing, and nyquist frequency will be shown. The result can be for all ganglion cells or
   only midgets. The visual field can be either that of the right eye, or both eyes combined as a mean, or a total, or a maximum density.
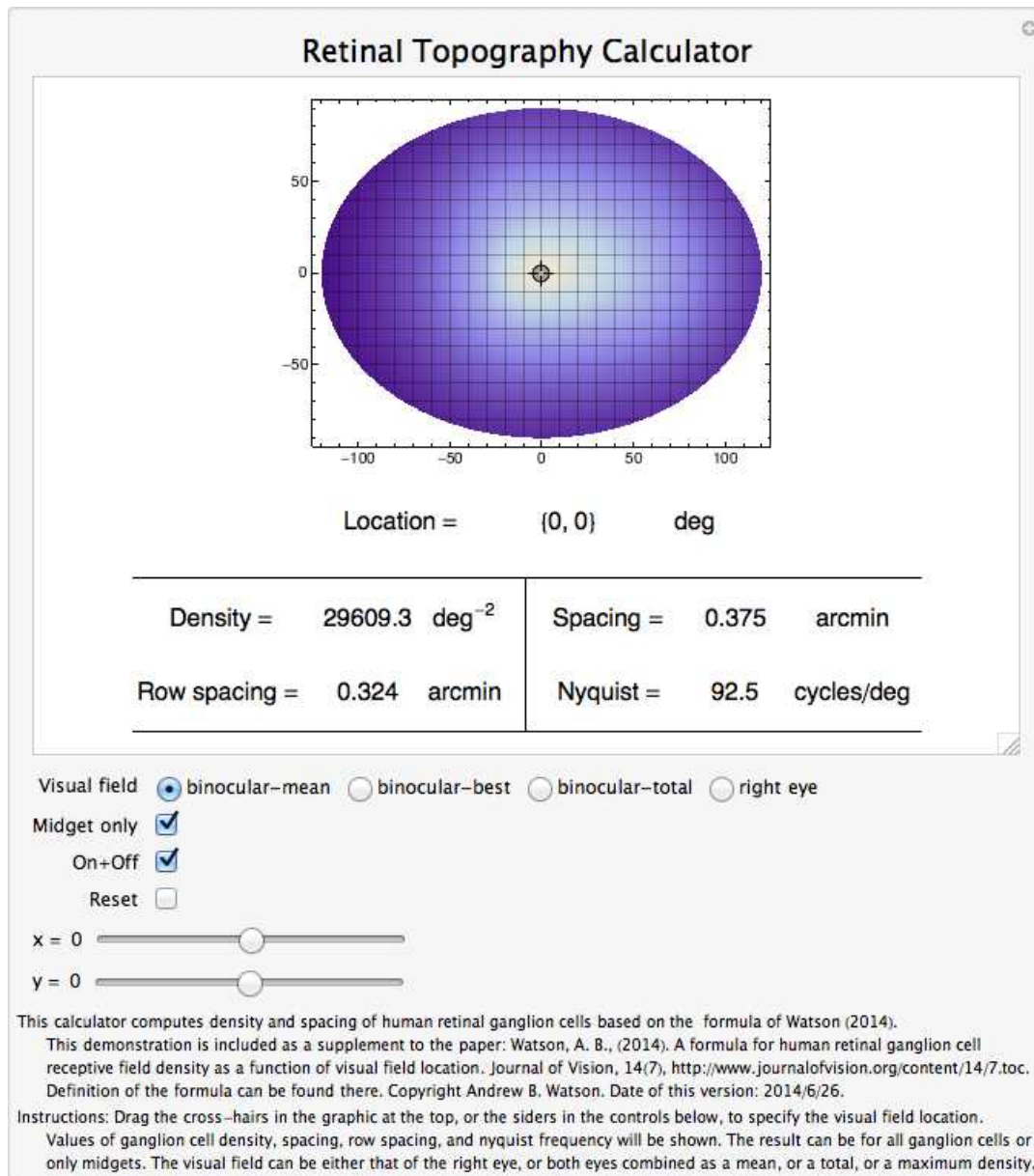
Figure 19. Demonstration of Retinal Topography Calculator.

Appendix 1: Demonstration

As a supplement to this paper we provide an interactive calculator that returns density and spacing at arbitrary visual field locations. The demonstration requires the use of the Wolfram CDF player, available at https://www.wolfram.com/cdf-player/. An illustration of the calculator is shown in Figure 19.

Appendix 2: Mathematica tables and functions

As a supplement we provide a Mathematica Notebook that contains a number of tables and functions derived and used in this report. The Notebook is a text file, but is most readable using the free Wolfram CDF Player available at https://www.wolfram.com/cdf-player/.

Appendix 3: Notation

The following is a table of notation used in this report.

Symbol	Definition	Unit
r	Eccentricity in deg relative to the visual axis	deg
k	Meridian index	
$d(r, k)$	Density of cells or receptive fields at eccentricity r along meridian k	deg^{-2}
$s(r, k)$	Spacing between receptive fields at eccentricity r along meridian k	deg
c, g, m, gf, mf	Subscripts to indicate cones, RGC, mRGC, RGCf, and mRGCf	
$h(r)$	Displacement of RGC from RGCf at eccentricity r	deg
$f(r)$	Fraction of RGC that are midget, as a function of eccentricity	dimensionless
Δ_k	Offset between optic and visual axis along the specified meridian	mm
r'	Eccentricity in deg relative to the optic axis	deg
r_{mm}	Eccentricity in mm relative to the visual axis	mm
r'_{mm}	Eccentricity in mm relative to the optic axis	mm
N	Nyquist frequency of hexagonal lattice	cycles/deg
S	Point spacing of hexagonal lattice	deg
R	Row spacing of hexagonal lattice	deg
D	Point density of hexagonal lattice	deg^{-2}

Table A1. Notation.

Appendix 4: Formula parameters and useful numbers

Item	Value	Unit
Peak cone density	14,804.6	deg^{-2}
Peak RGCf density	33,162.3	deg^{-2}
Peak mRGCf density	29,609.2	deg^{-2}
Minimum on-center mRGCf (or cone) spacing	0.5299	arcmin
Peak on-center mRGCf (or cone) Nyquist	65.37	cycles/deg
$f(0)$, midget fraction at zero eccentricity	$1/1.12 = 0.8928$	
r_m, scale factor for decline in midget fraction with eccentricity	41.03	deg

Table A2. Formula parameters and useful numbers.

Appendix 5: Density, spacing, row spacing, and Nyquist frequency

At least in the fovea, both photoreceptors and midget ganglion cell receptive fields form an approximately hexagonal lattice. Because we will make use of these formulas in the text, we review here the relationships among various metrics of a hexagonal lattice of points: $S(\mathrm{deg})$ = the spacing between adjacent points, $R(\mathrm{deg})$ = the spacing between rows of points, $D(\mathrm{deg}^{-2})$ = the density of points, and $N(\mathrm{c/deg})$ = the Nyquist frequency of the lattice (the highest frequency that can be supported by a particular row spacing). These formulas will allow us to convert among these metrics. Then

$$R = \frac{\sqrt{3}S}{2} = \sqrt{\frac{\sqrt{3}}{2D}} = \frac{1}{2N} \tag{A1}$$

$$D = \frac{1}{RS} = \frac{\sqrt{3}}{2R^2} = \frac{2}{\sqrt{3}S^2} = 2\sqrt{3}N^2 \tag{A2}$$

$$N = \frac{1}{2R} = \frac{1}{\sqrt{3}S} = \sqrt{\frac{D}{2\sqrt{3}}} \tag{A3}$$

$$S = \sqrt{\frac{2}{\sqrt{3}D}} = \sqrt{\frac{1}{3N}} = \frac{2R}{\sqrt{3}} \tag{A4}$$

Appendix 6: Conversion formulas for retinal dimensions

Conversion of eccentricities in millimeters to degrees

Eccentricity is defined as distance from a visual center. Anatomical measurements of the retina often express eccentricity in millimeters. We would like to convert these measurements to degrees of visual angle (deg) relative to the visual axis. Drasdo and Fowler (1974) used a model eye to compute conversions from retinal distances in millimeters to degrees. Their presentation does not, however, provide analytical expressions of the relevant quantities, so we must derive them from the figures. In their figure 2 they show a "curve showing computed relationship between retinal arc lengths and visual angles from the optic axis." We have extracted the contour and fit it with a third order polynomial,
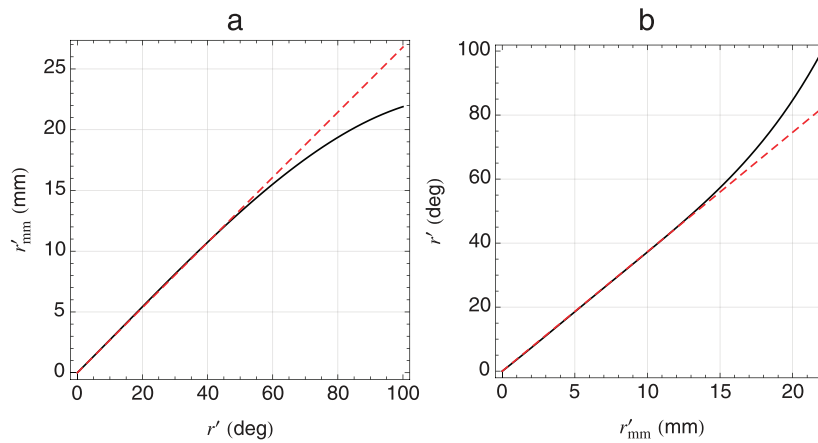
Figure A1. Relation between retinal distance from the optic axis in millimeters and degrees. The linear approximations shown as red dashed lines have slopes of 0.268 and 3.731, respectively.

$$r'_{mm}(r') = 0.268r' + 0.0003427r'^2 - 8.3309*10^{-6}r'^3$$

$$\text{(A5)}$$

In this equation, r'_{mm} refers to distance in mm, while r' is the comparable measurement in degree. The prime marking indicates a measurement relative to the optic axis.

We use this equation to translate optical eccentricities in degrees to millimeters. It is plotted in Figure A1a, along with a linear function with slope 0.268. The linear approximation is acceptable up to angles of 40°. We also fit to the transpose of the contour data, to obtain an inverse function,

$$r'(r'_{mm}) = 3.556r'_{mm} + 0.05993'^2_{mm} - 0.007358'^3_{mm}$$
$$+ 0.0003027'^4_{mm}$$

$$\text{(A6)}$$

We use this function, shown in Figure A1b, to convert optical eccentricities in millimeters to degrees. Dacey (1993) used a second order polynomial here, but its fit is poor at very small (0 mm) or large (22 mm) eccentricities. The linear approximation shown in the figure has a slope of $1/0.268 = 3.731$.

Conversion of mm² to deg²

The preceding formulas convert eccentricities (distances) from millimeters to degrees. We also need to convert local areas from mm² to deg². In their figure 5, Drasdo and Fowler (1974) show "variation of retinal area per solid degree with peripheral angle from the optic axis." We have fit this with a polynomial

$$a(r') = 0.0752 + 5.846 \times 10^{-5}r' - 1.064 \times 10^{-5}r'^2$$
$$+ 4.116 \times 10^{-8}r'^3$$

$$\text{(A7)}$$

where a is the ratio of areas mm²/deg². We have used this to convert cell densities in mm⁻² to deg⁻². The function is illustrated in Figure A2.

Visual versus optical axis

Drasdo and Fowler's (1974) angular measurements are relative to the optic axis. Measurements of cone densities and psychophysical predictions are usually expressed relative to the visual axis. According to Charman (1991), quoting Emsley (1952), the optical axis intersects the retina 1.5 mm nasal and 0.5 mm superior to the visual axis. In the visual field, the optical center is thus 1.5 mm temporal of the visual center. To convert eccentricities from millimeters relative to the visual axis to degrees relative to the visual axis, we use the following approximation

$$r(r_{mm}, m) = r'(r_{mm} - \Delta_m) + r'(\Delta_m) \qquad \text{(A8)}$$
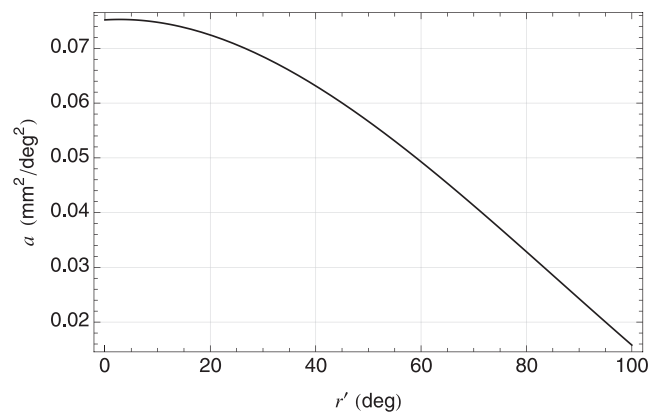
where m is the index of the meridian, and the

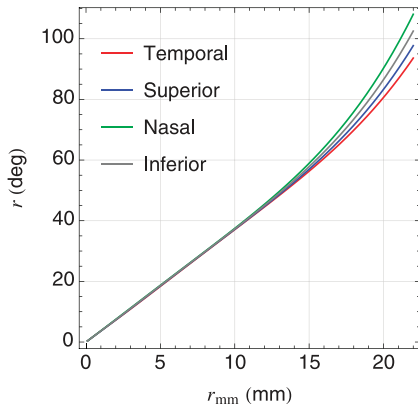Figure A2. Area ratio as a function of angular distance from the optic axis.

Figure A3. Relation between distance from the visual axis in millimeters and degrees, with correction for offset between visual and optic axes.

Figure A4. Eccentricities in degree computed with and without correction for offset between visual and optic axes.

corresponding offsets Δ from optic to visual axis in mm are given by

$$\Delta = \begin{bmatrix} 1.5 & .5 & -1.5 & -.5 \end{bmatrix}. \qquad (A9)$$

We remind that primed eccentricities are relative to the optic axis. The relation between visual millimeters and visual degrees for the four meridians is shown in Figure A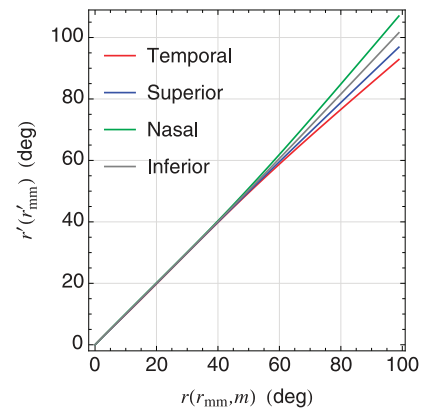3. Note that without the correction of visual-optical offset, all curves would be superimposed and look like Figure A1b above.

In Figure A4 we show the relation between eccentricities in degrees computed with and without the correction for the offset. Each curve is a parametric plot, where the millimeter argument is relative to either optical or visual axis. The correction is only significant above 40°.